HHS Public Access

Author manuscript

ACS Chem Biol. Author manuscript; available in PMC 2016 May 15.

Published in final edited form as:

ACS Chem Biol. 2015 May 15; 10(5): 1278–1289. doi:10.1021/cb5010367.

Rapid Synthesis, RNA Binding, and Antibacterial Screening of a Peptidic-Aminosugar (PA) Library

Liuwei Jiang[†], **Derrick Watkins**[‡], **Yi Jin**[†], **Changjun Gong**[†], **Ada King**[‡], **Arren Z. Washington**[§], **Keith D. Green**[‖], **Sylvie Garneau-Tsodikova**[‖], **Adegboyega K. Oyelere**[§], and **Dev P. Arya**[*,†,‡]

[†]Laboratory of Medicinal Chemistry, Department of Chemistry, Clemson University, Clemson, South Carolina 29634, United States

[‡]NUBAD, LLC, Greenville, South Carolina 29605, United States

[§]School of Chemistry and Biochemistry, Georgia Institute of Technology, Atlanta, Georgia 30332, United States

[‖]College of Pharmacy, Department of Pharmaceutical Sciences, University of Kentucky, Lexington, Kentucky 40536-0596, United States

Abstract

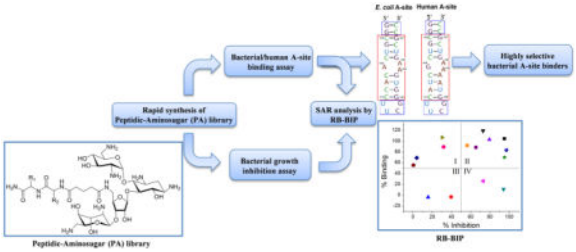

A 215-member mono- and diamino acid peptidic-aminosugar (PA) library, with neomycin as the model aminosugar, was systematically and rapidly synthesized via solid phase synthesis. Antibacterial activities of the PA library, on 13 bacterial strains (seven Gram-positive and six Gram-negative bacterial strains), and binding affinities of the PA library for a 27-base model of the bacterial 16S ribosomal A-site RNA were evaluated using high-throughput screening. The results of the two assays were correlated using Ribosomal Binding-Bacterial Inhibition Plot (RB-BIP) analysis to provide structure–activity relationship (SAR) information. From this work, we have identified PAs that can discriminate the *E. coli* A-site from the human A-site by up to a 28-fold difference in binding affinity. Aminoglycoside-modifying enzyme activity studies indicate that APH(2″)-Ia showed nearly complete removal of activity with a number of PAs. The synthesis of the compound library and screening can both be performed rapidly, allowing for an iterative

[*]Corresponding Author: Telephone: 1-864-656-1106. Fax: 1-864-656-6613. dparya@clemson.edu.

Supporting Information: High-throughput bacterial screening results, selected compounds NMR characterizations, NMR spectrum, and mass spectrometry results are available free of charge via the Internet at http://pubs.acs.org.

Notes: The authors declare the following competing financial interest(s): DPA has ownership interest in NUBAD LLC.

process of aminoglycoside synthesis and screening of PA libraries for optimal binding and antibacterial activity for lead identification.

Aminoglycoside antibiotics, e.g., amikacin, gentamicin, kanamycin, and neomycin, are a class of clinically significant chemotherapeutics, which have broad-spectrum activities against both Gram-negative and Gram-positive bacteria.[1,2] Aminoglycosides inhibit bacterial growth by binding to the A-site decoding region of the bacterial 16S rRNA within the 30S ribosomal subunit. A-site binding by aminoglycosides leads to mistranslation of mRNA or premature termination of protein synthesis. The loss of protein translational fidelity results in the death of bacteria.[3–6]

Emergence of drug resistance has become a public problem in applying aminoglycoside antibiotics in the therapy of bacterial infections.[1,7] In response to the requisite but still deficient rRNA binding affinity research, an approach for a comprehensive study of the binding and antibacterial activity of aminoglycoside-small molecule conjugates is urgently needed. A common strategy is used in the aforementioned studies to improve antibacterial activity: maintaining the backbone of aminoglycosides but adding additional recognition/binding elements. Schweizer et al. showed that amphiphilic neomycin-peptide/aromatic ring conjugates with triazole or amide linkages on the 5″ position exhibit better activity than neomycin against neomycin-resistant strains.[8–10] Substitution of the 5″-OH group of neomycin with mono- or disaccharides also has shown improved activity compared to that of neomycin against neomycin-resistant strains.[11–13] These previous studies produced compounds with improved binding affinity to rRNA and more potent antibacterial activity than the original aminoglycosides.[13]

Amino acids (natural and unnatural) that can comprise peptides have various chemical structures, polarity, electrical charges, and hydrophobicity/hydrophilcity resulting in diverse biological activity. Some peptides are known for their ability to interact with microbial lipid membranes, resulting in destabilization, translocation, pore formation, or lysis of microorganisms.[14,15] A number of cationic amphiphilic peptides are found to have the ability to traverse intact cytoplasmic membranes to interact with internal targets.[16] The chemical diversity of amino acids, their ability to form contacts with ribosome RNA and protein constituents, and their ability to regulate uptake across the bacterial membrane makes them perfect moieties for conjugation to enhance the A-site binding affinity and/or antibacterial activity of aminoglycosides. The ribosome (RNA and peptides) offers a multitude of sites for interaction with the peptide-linked aminosugars. Moreover, newer targets for aminoglycosides are being discovered, further enhancing the need for efficient and rapid methods for their synthesis and evaluation.[17–21]

Recent studies have shown increased antibacterial activities upon conjugation of aminoglycosides with small molecules, as demonstrated by improvement in MICs; however, the majority of these studies have not provided binding information describing the ligand–target interaction (aminoglycoside–rRNA).[8,9,13,22–24] Recently, a single concentration assay was adapted to screen compound libraries for antibacterial activity. The results of the assay were well correlated with antibacterial activity of bacterial strains determined by MIC calculations.[18]

Antibacterial activity was correlated with data reporting on binding to the ribosomal A-site to provide information about the possible mechanism of action. The A-site binding data were determined from a fluorescent probe displacement assay that can be performed rapidly to screen large libraries of compounds in a high-throughput format.[18,19] The A-site binding affinity and antibacterial activity from the compound library can be rapidly analyzed by Ribosomal Binding-Bacterial Inhibition Plots (RB-BIP). Using the RB-BIP here, we correlate the antibacterial activity to the A-site binding affinity of compound libraries. We have successfully employed RB-BIP to analyze a neomycin dimer library in a previous study.[18] With RB-BIP, the amino-acid-neomycin library will provide important structure–activity relationship (SAR) information with which aminoglycoside-based lead compounds may be designed.

The solution phase synthesis of aminoglycoside conjugates, utilized in studies to date,[25–34] have limited the number of compounds that can be synthesized and studied. A library approach to screening requires a rapid method for conjugation of required moieties to the aminoglycoside. Here, we show that 215 peptidic-aminosugars (PAs) with mono- and diamino acids were rapidly synthesized by using neomycin and 14 amino acids via solid phase synthesis. We also report a SAR analysis of A-site binding and antibacterial activity for amino acid-neomycin conjugated PAs. Because the synthesis, screening, and analysis can be performed rapidly, we have employed RB-BIP analysis for every compound in the library. The synthesis and screening approach described here is amenable to the development of larger and more diverse aminoglycoside modifications using solid phase synthesis. Coupled with rapid screening approaches presented here, the identification of useful hits can be rapidly performed.

Results and Discussion

Synthesis of a Neomycin PA Library

A 215 PA library containing mono- and diamino acid conjugated neomycin was rapidly synthesized by modifying the standard 9-fluorenylmethoxycarbonyl (Fmoc)-based solid-phase peptide synthesis protocol (Scheme 1).[35] Fourteen L-amino acids (*β*-alanine, arginine, asparagine, aspartic acid, cysteine, histidine, leucine, phenylalanine, proline, serine, threonine, tryptophan, tyrosine, and valine) were studied in the full library. In addition to the full library, five lysine-neomycin conjugates were synthesized for comparison with arginine-neomycin compounds. Protected 5″-amino-neomycin (1) was synthesized by modifying previous methods.[36–39] A glutaric anhydride reaction with 5″-amino-neomycin yielded the amide bond linked monomer 2 required for solid-phase synthesis (Scheme 1). Due to presence of the large *tert*-butoxycarbonyl (Boc) group, as observed via characteristic resonances in proton NMR spectra, compound **2** was deprotected to remove all Boc groups before NMR characterization. This modified method is capable of synthesizing hundreds of PAs in a short time, on small scales with low costs and minimal labor. The ribosomal A-site binding affinity and bacterial growth inhibition were then examined for all 215 compounds in the library.

Screening of the Peptide-Neomycin Conjugate Library for A-site Binding

The peptide-neomycin compound library was screened for A-site binding affinity using a high-throughput assay previously developed in our laboratory.[19] This method is a fluorescence-based competition assay, which uses a 27-base RNA model of the ribosomal A-site and a fluorescent reporter molecule, F-neo (Figure 1). The fluorescence of F-neo increases when competitively displaced by an A-site binding compound. This screening technique is used for measuring the relative binding affinity of a compound library compared to neomycin (Figure 1C). The assay was validated for A-site binding by determining the relative displacement of known aminoglycosides with previously reported results;[40] additionally, the assay has been successfully employed in screening of a neomycin dimer compound library.[18]

Data collected for the single amino acid-neomycin conjugates demonstrated that the A-site has a strong preference for neomycin conjugated to positively charged amino acids, such as arginine and lysine—These conjugates have binding affinities for the A-site that is greater than that of neomycin alone (Table 1). Polar residues, overall, reduce the affinity of neomycin less than nonpolar residues, with cysteine maintaining a moderate binding affinity for the A-site while serine and asparagine have half the original affinity of neomycin. With the exception of β-alanine, all nonpolar amino acids resulted in a reduction of neomycin binding below 50% when conjugated to neomycin. The hydrophobic aromatics of phenylalanine and tyrosine reduce the binding of the conjugated neomycin to 33% of the nonconjugated neomycin, while the more polar tryptophan only reduces the binding to 62%. The negatively charged aspartate is the most detrimental residue to binding, reducing the conjugate to 14% binding of the nonconjugated neomycin.

The docking of compounds into the ribosomal A-site suggests that the amino acid conjugated to neomycin may alter the orientation of the rings on the aminoglycoside—Docking of neomycin alone results in an orientation of the aminoglycoside rings that is similar to that of the crystal structure of neomycin bound by the *E. coli* ribosomal A-site (Figure 2).[41] However, the addition of the amino acid side chain to neomycin results in an alternate conformation of ring I and ring II as well as the positioning of the amino acid side chain between rings III and IV and the floor of the RNA groove. Future structural work will determine the relevance of the calculations for the binding of the amino acid conjugates, but these results indicate that the introduction of the amino acid side chain to neomycin introduces alternate binding modes to the aminoglycoside.

The diamino acid conjugates prefer only a single positive charge, cysteine or aromatic residues—An arginine at position 1 results in three diamino acid conjugates with higher affinity than that of the nonconjugated neomycin, with NeoRW binding 20% higher. Three of the four lysine diamino acid conjugates have affinity almost equivalent to or greater than that of neomycin. However, arginine at postion 2 has negative effects on the binding of most compounds, indicating that consecutive positive charges diminish binding affinity. Cysteine also appears to be beneficial for binding in the diamino acid conjugates, with three compounds binding better than neomycin when cysteine is present at position 1, including the highest affinity compound, NeoCY.

A tryptophan at position 1 has the most consistent positive effect on the binding of the diamino acid conjugates. Despite the fact that the monoamino acid of tryptophan has diminished binding compared to the nonconjugated neomycin, four of the conjugates have greater affinity than the nonconjugated neomycin, four of the conjugates have reduced affinity of 15% or less, and only three of the conjugates with tryptophan at position 1 have the affinity reduced by more than 50%. Although the aromatic nature of tryptophan would indicate that stacking interactions are important, the presence of the other aromatic compounds, phenylalanine and tyrosine, reduces the affinity of all the diamino acid conjugates with most having over 50% reduction in affinity compared to neomycin. This observation indicates that the size and/or presence of the amine of tryptophan contribute to the affinity of the conjugates.

The presence of the negatively charged aspartate is detrimental to binding when present in the monoamino acid conjugate, or when present at position 1 or position 2 in the diamino acid conjugates. The electrostatic repulsion between aspartate with the phosphate backbone likely precludes the presence of any negatively charged residues for RNA binding in the small chain of amino acids.

The conjugation of amino acids to neomycin increases the difference in the affinity of the aminoglycoside between the E. coli and the human ribosomal A-site models—Previous work has been shown that there is approximately a 5-fold difference in the affinity of neomycin for the human A-site model and the *E. coli* model.[42] The screening of the compound library for F-neo displacement from the human A-site identified compounds that discriminate between the two models. The results of the screen were confirmed for two of the identified compounds, NeoWL and NeoYW, by determining the IC_{50} for the compound displacement of F-neo from each site. Each of these compounds has a greater difference in binding affinity for the *E. coli* A-site and the human A-site than that of neomycin, with NeoWL having almost a 15-fold greater affinity of the *E. coli* A-site and NeoYW having almost a 30 fold greater affinity for the *E. coli* A-site. The identification of a compound that can discriminate between A-sites indicates that the conjugation of amino acids has the potential to produce compounds that are highly specific for the rRNA target (Figure 3).

The Screening of the PA Library for Bacterial Growth Inhibition

The bacterial growth inhibition of the neomycin PA library was determined by using a single concentration high-throughput screen (HTS) that was developed by De La Fuente et al.[43] This screening method has been used in our laboratory to identify compounds with antibacterial activity and was validated by determining MIC of the compounds.[44] Antibacterial HTS was performed on seven Gram-positive bacterial strains (*Staphylococcus aureus* ATCC 25923, *S. aureus* NorA,[45] methicillin-resistant *S. aureus* (MRSA) ATCC 33591, *Listeria monocytogenes* ATCC 19115, *Streptococcus pyogenes* ATCC 12384, *Enterococcus faecalis* ATCC 49533, *E. faecalis* ATCC 700802) and six Gram-negative bacterial strains (*Escherichia coli* ATCC 25922, *E. coli* TolC,[45] *Enterobacter cloacae* ATCC 13047, *Serratia marcescens* ATCC 13880, *Pseudomonas aeruginosa* ATCC 27853, *Acinetobacter baumannii* ATCC 19606) for all PA at 5 μM. The resulting data are presented

in the Supporting Information in detail with errors associated with each measurment (Table S1). The amino acid preferences on bacterial growth inhibition are summarized in Table 2. Results of *S. pyogenes* ATCC 12384, *E. faecalis* ATCC 29533, *E. faecalis* ATCC 700802, and *A. baumannii* ATCC 19606 are omitted from the table due to negligible bacterial growth inhibition.

In order to define amino acid preferences at position 1 and at position 2 in the neomycin conjugates, we analyzed the inhibition data based on the average standard deviation (σ) for all compounds with specific residue at position 1 or position 2 above the mean of inhibition of all compounds for a specific bacterial strain—The average inhibition and standard deviation from the mean for all compounds was first determined for each strain. The average inhibition was found for each class of compounds NeoYX or NeoXY, where Y is a specific amino acid and X is varied across all amino acids used in the conjugation. The average for each class was divided by the standard deviation of all conjugates to determine the number of σ above or below the mean for each class of compounds that inhibited the growth of each strain. This treatment allows us to determine a quantitative measurement of the preferred amino acid at each position.

The inhibition of amino acid conjugates on bacterial growth shows a strong preference for the positive amino acids arginine and lysine—The NeoR and NeoK conjugates show the broadest impact of all amino acid conjugates at position 1, with the average over 1σ above the mean for six of the 10 strains tested for NeoRX and three of the 10 strains tested for NeoKX. NeoRX compounds were favored approximately 2σ above the mean for Gram-positive bacterial strains *S. aureus* ATCC 25923, *S. aureus* NorA, and *L. monocytogenes* ATCC 19115. NeoRX was also favored 2σ above the mean for Gram-negative bacterial strains *E. coli* ATCC 25922, *E. cloacae* ATCC 13047, and *S. marcescens* ATCC 13880 and 0.78σ above the mean for *E. coli* TolC. NeoKX compounds were favored over 1σ above the mean for Gram-positive bacterial strains *S. aureus* NorA and *L. monocytogenes* ATCC 19115 and Gram-negative bacterial strains *E. coli* TolC and *E. cloacae* ATCC 13047 and 2.13σ above the mean for *E. coli* ATCC 25922.

Both cysteine and tryptophan amino-acid-neomycin derivatives, NeoCX and NeoWX, were also broadly effective in inhibiting the strains, with both classes of compounds being the only derivatives that were significantly above the mean for inhibiting the Gram-negative *P. aeruginosa* ATCC 27853. The NeoCX conjugates appear more selective toward the Gram-positive strains, inhibiting *S. aureus* ATCC 25923, *S. aureus* NorA, and *L. monocytogenes* ATCC 19115 by over 0.5σ. In addition to *P. aeruginosa* ATCC 27853, NeoWX conjugates also inhibit the Gram-negative strain *E. coli* TolC. Most significantly, NeoWX compounds were favored 1σ above the mean for inhibition of neomycin resistant MRSA ATCC 33591.

The amino acid at position 2 has less influence on inhibition compared to that of the amino acid at position 1. Only the NeoXW class of compounds appears to have a consistent influence on inhibition. NeoXW is favored over 1σ for the Gram-positive neomycin resistant MRSA ATCC 33591 and the Gram-negative *P. aeruginosa* ATCC 27853. NeoXW and NeoWX are the only class of the conjugates that are favored for both of these strains,

indicating that the presence of a tryptophan may influence mechanisms of resistance that arise in bacteria.

The results from the high-throughput antibacterial screen were further verified by MIC calculation of select compounds—We have previously shown that HTS at a single concentration for these strains is an excellent predictor of ligand antibacterial effects, as verified by MIC determinations. To verify the extrapolation of single point screening to MIC, we randomly picked a few ligands and determined their MIC values for select strains. MIC results show excellent correlation with single point determination (Table 3). For example, the MIC of NeoR was determined for *S. aureus* ATCC 25923 and MRSA ATCC 33591. In both cases, the MIC agreed with the results of the single point screen for NeoR, with NeoR having a MIC of 1.25 μM in *S. aureus* and inhibiting 95% growth in the single point screen. The MIC of NeoR in MRSA was determined to be >160 μM, which is also in agreement with the 2% inhibition observed in the single point screen.

Furthermore, the MIC was also determined for NeoRW for *S. aureus* ATCC 25923 and MRSA ATCC 33591. Consistent with the single point screen, the MIC for NeoRW was greater than that of NeoR in *S. aureus* at 10 μM and inhibited growth by 85% in the single point screen. The MIC for NeoRW was also found to be between 40 and 80 μM in MRSA. This compound inhibited the growth of MRSA by 45% in the single point screen and indicated that the single point screen is representative of the MIC of the compound for the neomycin resistant strain. Neomycin alone required >320 μM for complete inhibition of MRSA growth and showed negligible inhibition in the single point screen for this strain.

Correlating Ribosomal Binding Data and Bacterial Inhibition Data with RB-BIP Analysis

In order to rapidly draw structure activity relationships for the compounds tested, the data for both binding and inhibition assays of the PAs were plotted on RB-BIP. A similar assay has been used to correlate bacterial growth inhibition with translational inhibition.[46] RB-BIP analysis was performed on neomycin position 1 conjugates of arginine, cysteine, and tryptophan. A representative plot with arginine on conjugate position 1 from the two screens is shown in Figure 4, and the plots for the cysteine and tryptophan conjugates are given in the Supporting Information (Figures S1, S2). RB-BIPs outline the percent ribosomal binding of the compound as compared to neomycin on the *y* axis and the percent bacterial inhibition as compared to untreated cultures on the *x* axis. The RB-BIP can then be divided into quadrants I, II, III, and IV. Compounds plotted in quadrant II display both high binding to the ribosomal A-site and inhibition of bacterial growth. The correlation using the RB-BIP analysis for the PA compound library is similar to that observed by Wong et al. in correlating naturally occurring and bifunctional aminoglycosides, in which a linear relationship is observed between the MIC and translation inhibition. This correlation between binding and inhibition is similar to what we observe in quadrant II.[46] Compounds plotted in quadrant I exhibit strong binding to the model ribosomal A-site but weakly inhibit bacterial growth. Similar to previous work, the compounds in quadrant I could be correlated to transport limitations,[46] or other modes of resistance associated with ineffective binding. Quadrant III of the RB-BIP contains compounds with low ribosomal binding and inhibition of bacterial growth. Finally, quadrant IV shows compounds exhibiting inhibition of bacterial growth

with weak binding to the model A-site, which could have a different mode of action associated with the bacterial inhibition.[46]

As shown in Figure 4, the position 1 arginine conjugate that showed high bacterial growth inhibition (inhibition >50% at 5 μM) on neomycin susceptible Gram-positive bacterial strains (*S. aureus* ATCC 25923, *S. aureus* NorA, and *L. monocytogenes* ATCC 19115) are generally good A-site binding ligands, namely, NeoR, NeoRS, NeoRT, NeoRY, NeoRV, NeoRC, and NeoRW. The presence of a compound in or approaching quadrant II gives a strong SAR correlation between antibacterial activity and A-site affinity, indicating that the primary target of these conjugate molecules is likely the A-site of 16S rRNA. The same general trend is true for compounds against the neomycin susceptible Gram-negative strains *E. coli* ATCC 25922, *E. coli* TolC, *E. cloacae* ATCC 13047, and *S. marcescus* ATCC 13880 with the majority of the compounds falling in quadrant II. However, more of the compounds tend toward quadrant I for the Gram-negative strains than for the Gram-positive strains, indicating a preference for inhibition of Gram-negative strains.

Compounds NeoRN and NeoRR show up in quadrant IV of many of the bacterial strains. NeoRN has low A-site affinity but good bacterial growth inhibition on three out of seven neomycin susceptible bacterial strains. NeoRR showed very low A-site affinity (0% displacement on A-site screen) but good bacterial growth inhibition on *S. aureus* NorA, *L. monocytogenes* ATCC 19115, and *E. coli* TolC. From the RB-BIP, our model A-site is unlikely to be the target of NeoRN and NeoRR for inhibition of bacteria growth.

The NeoRW conjugate was the most effective compound against the neomycin resistant strains MRSA ATCC 33591 and *P. aeruginosa* ATCC 27853 as well as one of the strongest A-site binding compounds. Additionally, in the MRSA strain, it very closely approaches quadrant II. Its broad spectrum of activity and improved inhibition against neomycin-resistant strains makes NeoRW an attractive compound to use for expanding and further optimizing the PA library.

The translation inhibition ability of the 10 compounds active in the antimicrobial assays was tested in a cell-free translation inhibition assay—A number of these compounds (Table 4 and Table S13) are potent nanomolar inhibitors of protein synthesis, suggesting that these amino acid modifications do not adversely affect the ability of aminoglycosides to inhibit bacterial protein synthesis.

The 12 most promising PA conjugates were tested against a variety of aminoglycoside-modifying enzymes—The chosen enzymes included three regiospecific acetyltransferases,[47,48] a phosphotransferase,[49] and an acetyltransferase enzyme known to multiply acetylate aminoglycosides.[47] We can use the data obtained from the AME reactions to predict how the peptide-aminoglycoside conjugates might be modified in bacterial cells. The data presented in Figure 5 show that in almost all cases, the reactivity of the peptide-neomycin conjugate is reduced when compared to neomycin alone. The three regiospecific AACs, AAC(2′)-Ic, AAC(3)-IV, and AAC(6′)-Ie/APH(2″)-Ia (used solely for its acetylation activity), targeting the I and II rings show a reduction in rate of 50% or less with the exception of AAC(6′)-Ie/APH(2″)-Ia, with DPA1115 and DPA1229. However, this

is the most substrate- and cosubstrate-promiscuous of the three regiospecific AACs.[49] Eis was unaffected by the addition of the peptides to the neomycin structure; this is not all that surprising considering the large active site of the enzyme and its ability to acetylate neomycin three times. There was a reduction in activity with DPA1102, DPA1113, DPA1142, and DPA1285 with Eis. However, it should be noted that three of these compounds have a free thiol group (cysteine) that reacted with the indicators used for the acetyltransferase assay, and this decrease could be indicative of the consumption of indicator through this mechanism.

The most affected enzyme was APH(2″)-Ia, which showed nearly complete removal of activity with 8 of the 12 compounds. Since this enzyme is noted to modify the 3′ or 3‴ position of neomycin and other 4,5-DOS substituted aminoglycosides[50] rather than the actual 2″ position, the data indicate that modifying the 5″ position of neomycin with amino acids and peptides reduces the ability of neomycin to be phosphorylated by APH(2″)-Ia. While there was no singular compound that completely removed all activity of the modifying enzymes tested, it is possible that the reduction in the rate of modification could increase the time the unmodified PA conjugate is available to target the ribosome and perform its original function.

Conclusion

Large libraries of amino acid and aminosugar conjugated PAs can be rapidly synthesized via solid phase as an approach to find new effective broad-spectrum antibiotics. The analysis of the library identifies the residues that are preferred in the first two positions of an amino acid chain. The work presented here provides the first building block in the expansion of the library and identifies the optimal residues to further expand and optimize the peptide chain. Through rapid synthesis and screening, we identified PAs that bind strongly and selectively to the *E. coli* A-site model with up to 28 times greater affinity than to the model human A-site rRNA To the best of our knowledge, this is one of the most selective *E. coli* rRNA aminoglycoside ever reported, particularly for a neomycin class aminoglycoside, which is known to have very poor selectivity for bacterial over mammalian rRNA

The approach described in this work can identify compounds that correlate well between binding and growth inhibition, as well as those that bind well but do not inhibit the growth of bacteria. The resistance of bacteria to compounds that bind to the A-site may be a product of limited transport or a promiscuous enzyme. It has been previously shown that the RNA of the A-site is dynamic, and compounds that induce the destacking of A1492 and A1493 of the *E. coli* 16S rRNA result in mistranslation by the ribosome.[51–54] Further analysis of the high affinity compounds that do not inhibit bacterial growth can be followed by dynamic assays using 2-amino purine labeled RNA and an *in vitro* translation inhibition assay to assess the mode of resistance and help direct future modifications of these compounds.

The methodology for synthesizing, screening for both ribosomal binding and bacterial growth inhibition, and RB-BIP analysis of the data is a rapid, optimal approach that provides a systematic method for the rapid synthesis and screening of large aminoglycoside antibiotic libraries. The approach described here is expected to impact the analysis of modified aminoglycoside function against established and newly discovered targets, in addition to

assisting in the development of new leads for targeting bacterial, viral, and fungal pathogens that contain potential nucleic acid binding sites for these PAs.

Methods

Unless otherwise specified, chemicals were purchased from commercially available sources and used without further purification. NMR spectra were recorded on a Bruker Avance-500 spectrometer. MS (MALDI-TOF) spectra were recorded using a Bruker Daltonics/Miroflex MALDI-TOF spectrometer. *E. cloacae* ATCC 13047, *E. coli* ATCC 25922, *P. aeruginosa* ATCC 27853, *S. marcescens* ATCC 13880, and MRSA ATCC 33591 were purchased from the American Type Culture Collection (ATCC; Manassas, VA). *S. aureus* ATCC 25923 and *S. pyogenes* (ATCC 12384) were a gift from Dr. Tamara McNealy (Clemson University, Clemson, South Carolina). L. *monocytogenes* ATCC 19115, *E. faecalis* ATCC 700802, *E. faecalis* ATCC 49533, *A. baumannii* ATCC 19606, *S. aureus* NorA, and *E. coli* TolC were from Dr. Garneau-Tsodikova's laboratory (University of Kentucky). All culture supplies were purchased from Thermo Fisher Scientific (Pittsburgh, PA) and Sigma-Aldrich (St. Louis, MO).

Compound 1

Compound **1** was synthesized by modifying previously reported methods.[36–39] A mixture of neomycin sulfate (9.09 g, 10.0 mmol), Na_2CO_3 (13.78 g, 130.0 mmol), di-*tert*-butyl dicarbonate (28.37 g, 130.0 mmol), H_2O (480 mL), and CH_3OH (480 mL) was stirred at RT for 3 h. After removal of 500 mL of the solvent under reduced pressure, the solid was collected by filtration and washed with H_2O. The solid was then dried and purified by column chromatography using EtOAc/hexane/isopropanol (*v*/*v*, 90/30/3) as an eluent. Intermediate 1,3,2′,6′,2‴,6‴-hexa-*N*-(*tert*-butoxycarbonyl)-neomycin was obtained as a white solid in 61% yield (7.41 g). Intermediate 1,3,2′,6′,2‴,6‴-hexa-*N*-(*tert*-butoxycarbonyl)-neomycin (4.86 g, 4.0 mmol) was then dissolved in dry pyridine (40 mL). To the above solution, 2,4,6-triisopropylbenzenesulfonyl chloride (TPSCl; 9.69 g, 32.0 mmol) was added. The reaction mixture was stirred at RT for 41 h and was then neutralized with saturated $NaHCO_3$. The turbid liquid was extracted with EtOAc, and the organic layer was washed with saturated NaCl, aqueous HCl (0.5 M; two times), saturated $NaHCO_3$, and H_2O. After solvent evaporation, the solid was then purified by column chromatography using CH_2Cl_2/CH_3OH/EtOAc (v/v, 100/3/3) as an eluent. Intermediate 1,3,2′,6′,2‴,6‴-hexa-*N*-(*tert*-butoxycarbonyl)-5″-*O*-(2,4,6-triisopropylbenzenesulfonyl)-neomycin was obtained as a white solid (3.08 g, 51%). A mixture of 1,3,2′,6′,2‴,6‴-hexa-*N*-(*tert*-butoxycarbonyl)-5″-*O*-(2,4,6-triisopropylbenzenesulfonyl)-neomycin (1.46 g, 0.98 mmol), NaN_3 (0.96 g, 14.7 mmol), and *N*,*N*-dimethylformamide (DMF; 15 mL) was stirred for 12 h at 80 °C. The mixture was then extracted with EtOAc and washed with H_2O. After solvent removal, 1,3,2′,6′,2‴,6‴-hexa-*N*-(*tert*-butoxycarbonyl)-5″-azido-neomycin was obtained as a white solid in 96% yield (1.17 g). 1,3,2′,6′,2‴,6‴-Hexa-*N*-(*tert*-butoxycarbonyl)-5″-azido-neomycin (500 mg, 0.4 mmol) was dissolved in ethanol (5 mL) and mixed with Pd/C (10 wt % on activated carbon; 250 mg). The mixture was stirred under a hydrogen atmosphere for 12 h at RT. Pd/C was removed by filtration, and the filtrate was concentrated by vacuum.

The crude product was then purified by column chromatography using CH_2Cl_2/CH_3OH (v/v, 100/5) as an eluent. Compound **1** was obtained as white solid in 90% yield (440 mg).

Compound 2

To a DMF solution (10 mL) of compound **1** (1.00 g, 0.82 mmol), glutaric anhydride (86.1 mg, 0.86 mmol) and triethylamine (TEA) (120 μL, 0.86 mmol) were added dropwise. The resulting solution was stirred at RT for 30 min before dilution with 50 mL of EtOAc. The EtOAc layer was washed with 0.01 M HCl solution (50 mL) followed by washing with water (100 mL × 3) and brine (50 mL) and then was dried with anhydrous Na_2SO_4. The crude product was stirred in ethanol (10 mL) and a K_2CO_3 (1.0 g) mixture for 4 h and diluted with 50 mL of EtOAc. The EtOAc layer was washed with 0.01 M HCl solution (50 mL) followed by washing with water (100 mL × 3) and brine (50 mL) and then dried over anhydrous Na_2SO_4. The solution was concentrated in a vacuum affording compound **2** as a light yellow solid in 95% yield (1.1 g).

Deprotection of Compound 2

To 500 μLofTFA/water (v/v 90/10) solution, 30 mg (22.6 mmol) of compound **2** was added. The resulting solution was decanted into 10 mL of ice-cold diethyl ether after stirring at RT for 2 h. White precipitate formed in ether was collected by centrifugation and dried by a vacuum to afford 30 mg of a light yellow solid. Yield = 98%. ^{1}H NMR (500 MHz, D_2O): δ 5.88 (d, J = 3.8 Hz, 1H), 5.35 (d, J = 4.2 Hz, 1H), 5.26 (s, 1H), 4.35 (t, J = 4.8 Hz, 1H), 4.29–4.26 (m, 1H), 4.25–4.21 (m, 1H), 4.21–4.17 (m, 2H), 4.07 (t, J = 9.6 Hz, 1H), 3.98 (t, J = 9.7Hz, 1H), 3.95–3.91 (m, 1H), 3.91–3.87 (m, 1H), 3.79 (d, J = 1.1 Hz, 1H), 3.72–3.65 (m, 2H), 3.56 (s, 1H), 3.54–3.47 (m, 3H), 3.45–3.28 (m, 6H), 2.48–2.44 (m, 1H), 2.38 (t, J = 7.4 Hz, 2H), 2.29 (t, J = 7.5 Hz, 2H), 1.93–1.80 (m, 3H). ^{13}C NMR (126 MHz, D_2O): δ 177.97, 176.60, 163.35, 163.07, 162.79, 162.51, 119.95, 117.63, 115.31, 112.99, 109.32, 95.93, 95.06, 85.08, 81.07, 77.56, 75.25, 73.72, 72.38, 70.43, 70.26, 69.98, 68.18, 67.66, 67.50, 53.32, 50.95, 49.64, 48.65, 40.94, 40.58, 40.09, 34.92, 33.14, 27.97, 20.78. MS (MALDITOF) m/z calcd for $C_{28}H_{54}N_7O_{15}$ $[M + H]^+$: 728.4. Found: 728.3.

General Procedure for the Solid Phase Synthesis of PA Library

Coupling of Amino Acids—Rink amide MBHA resin (5.08 mg) with 0.59 mmol/g loading was swollen in DMF (2 mL, 2 ×1 min) with a constant stream of nitrogen bubbling before Fmoc deprotection. Resin was deprotected by mixing with 25% piperidine in DMF (2 mL, 2 × 5 min). *N*-Fmoc protected amino acids (5 equiv) were then coupled to resin in DMF in the presence of HCTU (5 equiv) and DIPEA (10 equiv) for 1 h. Resin was washed extensively with DMF (4 × 1 mL) between reactions, and the reaction was tested for completeness via Kaiser test.

Coupling of Compound 2—After amino acid couplings were completed, resin was deprotected with 25% piperidine in DMF (2 mL, 2 × 5 min) and then washed extensively with DMF (4 × 1 mL). Compound **2** (3 equiv) was coupled in NMP in the presence of HCTU (3 equiv) and DIPEA (5 equiv) for 24 h. After coupling, resin was washed with DMF (4 × 1 mL) and CH_2Cl_2 (4 × 1 mL) and then was dried under room atmosphere for 1 h. Resin was stored under 0 °C before cleavage.

Side Chain Deprotection and Cleavage of PA from Resin

The PAs were cleaved from resin, and all protecting groups were removed by a 2 h treatment with 88:5:5:2 TFA/phenol/H_2O/TIPS (v/v; 150 μL). After the treatment, TFA was evaporated under nitrogen pressure. To the resulting resin, 600 μL of deionized water was then added to dissolve the cleaved PAs. The water layer was washed extensively with CH_2Cl_2 (500 μL) and EtOAc (3 × 500 μL) then lyophilized to afford final products as white powders. Final products were stored at −20 °C and protected from light and moisture.

General Procedure for Large-Scale Synthesis of Selected PA

Coupling of Amino Acids—Rink amide MBHA resin (19.9 mg) with 0.51 mmol/g loading was swollen in DMF (2 mL, 2 × 1 min) with stirring. Resin was deprotected by stirring with 25% piperidine in DMF (2 mL, 2 × 3 min). N-Fmoc protected amino acids (5 equiv) were then coupled to resin in DMF in the presence of HCTU (5 equiv) and DIPEA (10 equiv) for 1 h. Resin was washed extensively with and DMF (4 × 1 mL) between reactions and was tested for completeness via Kaiser test.

Coupling of Compound 2

After amino acid couplings were completed, resin was deprotected with 25% piperidine in DMF (2 mL, 2 × 5 min) and then washed extensively with DMF (4 × 1 mL). Resin was mixed with compound **2** (3 equiv) in DMF in the presence of HCTU (3 equiv) and DIPEA (5 equiv) for 24 h. After coupling, resin was washed with DMF (4 × 1 mL) and CH_2Cl_2 (4 × 1 mL) and then was dried under room atmosphere for 1 h. Resin was stored under 0 °C before side chain deprotection and cleavage.

Deprotection and Cleavage of PA from Resin

The PAs were cleaved from resin, and all protecting groups were removed by a 2 h treatment with 88:5:5:2 TFA/phenol/H_2O/TIPS (v/v; 500 μL). After deprotection, resin was removed from reaction mixture by filtration. Ice-cold diethyl ether (10 mL) was added into the filtrate to afford a white precipitate. The precipitated product was collected by centrifugation and washed with diethyl ether (3 × 1 mL) three times. The product was dried under a rough vacuum and lyophilized for 48 h to completely remove diethyl ether. The resulting final products were stored at −20 °C protected from light and moisture.

High-throughput Screening (HTS) of Antibacterial Activity and Determination of the Minimal Inhibitory Concentrations (MIC)

Antibacterial HTS and the determination of MIC were performed following a previously reported method.[43,55] *S. pyogenes*, *E. faecalis*, and *L. monocytogenes* were cultured on Mueller Hinton (MH) agar with 5% lysed horse blood at 35 °C for 20 h and were then collected with a sterile cotton swab. The other bacteria were cultured in MH broth in a shaker–incubator at 37 °C for 20 h. The cultures were then diluted to an absorbance at 595 nm of 0.006 using sterile MH broth (lysed horse blood was added to *S. pyogenes*, *E. faecalis*, and *L. monocytogenes* strains after dilution, and the resulting blood concentration is 5%). The diluted bacteria aliquots were placed (90 μL per well) into 96-well clear flat bottom plates. For HTS, compounds (10 μL, 50 μM, in H_2O solution) were then added, and

the final concentration of the compounds was 5.0 μM. For the determination of MIC, compounds were diluted with water to give the following concentrations (800, 400, 200, 100, 50.0, 25.0, 12.5, 6.25 μM). The resulting solutions (10 μL) were then added to the 96-well plates, and the final concentrations of the compounds were 80, 40, 20, 10, 5.0, 2.5, 1.25, and 0.625 μM, respectively. Background controls (10 μL water and 90 μL MH broth solution), positive controls (a mixture of water (10 μL) and the diluted bacteria solution (90 μL)), and known drug controls (kanamycin, neomycin, gentamicin, and ampicillin) were run in each plate. In all plates, the absorbance at 595 nm was measured after 22 h incubations at 35 °C. The percentage bacterial growth inhibition was calculated as percentage inhibition = 100−100 × ($A_{\text{testcompound}} - A_{\text{backgroundcontrol}}$)/($A_{\text{negativecontrol}} - A_{\text{backgroundcontrol}}$). In cases where treatment appeared to enhance the growth of the culture, inhibition was scored as zero rather than negative inhibition. The MIC is determined to the lowest (minimum) concentration at which no visible growth is present (percentage inhibition ≥99%).

Ribosomal RNA A-site Binding

The described compound library was screened using an F-neo competitive binding assay as described in detail by Watkins et al.[40] In short, the displacement assay was performed in duplicate with each compound at a 0.3 μM concentration to 0.1 μM F-neo:A-site complex using 100 reads per well at an excitation/emission of 485/535 nm. All experiments were performed in 10 mM MOPSO (pH 7.0), 50 mM NaCl, and 0.4 mM EDTA The displacements of F-neo by test compounds were determined by the increase of fluorescence measured after the addition of the test compound to wells of a 96-well plate containing F-neo A-site complex compared to the fluorescence of the F-neoA-site complex alone (Δ*F*). Percent binding was calculated from the ratio of the change in fluorescence by the addition of the test compound (ΔF_{Drug}) with the change in fluorescence by the addition of neomycin (ΔF_{Neo}), using eq 1:

$$\%\text{binding} = (\Delta F_{\text{drug}}/\Delta F_{\text{neomycin}}) \times 100\% \quad (1)$$

All dockings were performed as blind dockings using Autodock Vina 1.0.[56] Docking was performed using an “exhaustiveness” value of 12. All other parameters were used as a default. All rotatable bonds within the ligand were allowed to rotate freely, and the A-site was kept rigid. Autodock Tools version 1.5.4[57] was used to convert the ligand and receptor molecules to the proper file formats for AutoDock Vina docking. All structures were visualized and images made using Pymol.[58]

The concentration of compound that displaces 50% of the F-neo (DC_{50}) of DPA1199 and DPA1308 was determined by the titration of each compound into 0.1 μM F-neo A-site complex containing either the *E. coli* or human model of the A-site, using 50 reads per well at an excitation/emission of 485/535 nm. All experiments were performed in duplicate in 10 mM MOPSO (pH 7.0), 50 mM NaCl, and 0.4 mM EDTA. The initial concentration range was 0.05 nM to 1 μM of each compound. The concentration was extended to 20 μM of each compound for the human A-site to obtain the DC_{50} due to a lack of saturation at the lower range. The DC_{50} was determined from the sigmoidal fit using Origin 5.0.

Cell Free Translation Assays

Working solutions were made of each compound using filtered *nano*Pure H_2O by serially diluting with final dose ranges of 1.25 μM to 2 nM for prokaryotic systems. *Escherichia coli* (*E. coli* S30 Extract System for Circular DNA, Promega, L1020) assays were performed as recommended by the manufacturer.[59,60] Briefly, varying concentrations of the compounds of interest were allowed to incubate in a solution of cellular extract and all amino acids for 20 min at RT. Following brief centrifugation, 0.40 μL of luciferase control template (Promega, L492A-C) was added to each tube. After gentle mixing and spin down, tubes were incubated at 37 °C for 60 min. Translation was terminated by inactivating on ice for 5 min. Upon returning to ambient temperature, 5 μL per tube was delivered to a LUMITRAC 200 96-well plate. Luminescence was immediately read following the addition of the luciferin solution using a Molecular Devices SpectraMax M2. IC_{50} values were determined by nonlinear fit using GraphPad Prism 6. All compounds were done in triplicate and standardized against an internal vehicle control.

Aminoglycoside-modifying Enzyme Activity

To determine if the PA compounds are enzymatically modified by aminglycoside-modifying enzymes, previously developed assays were employed to monitor the possible inactivation of these compounds.[47–49] All reactions were monitored at 25 °C (AAC(2′)-Ic, AAC(3)-IV, Eis, and APH(2″)) or 37 °C (AAC(6′)-Ie/APH(2″)-Ia) on a SpectraMax M5 microplate reader and performed in triplicate. All rates were normalized to neomycin (NEO).

Acetylation—The activity of several aminoglycoside acetyltransferases (AAC(6′)-Ie/APH(2″)-Ia, AAC(3)-IV, AAC(2′)-Ic, and Eis) was monitored using Ellman's method, coupling the release of CoASH with DTNB (ε = 14150 $M^{-1}cm^{-1}$) and monitored at 412 nm. Briefly, reactions (200 μL) contained PAs (100 μM), AcCoA (500 μM for Eis and 150 μM for all other acetyltransferases) and DTNB (2 mM) and were inititated with enzymes (0.125 μM AAC(3)-IV and AAC(2′)-Ic, 0.5 μM for all remaining acetyltransferases) in a corresponding buffer (100 mM sodium phosphate pH 7.4 for AAC(2′)-Ic, 50 mM MES pH 6.6 for AAC(6′)-Ie/APH(2″)-Ia and AAC(3)-IV, and 50 mM Tris pH 8.0 for Eis). Reactions were monitored taking measurements every 30 s for 30 min. Initial rates were calculated using the first 2–5 min of the reaction.

Phosphorylation—The phosphorylation of PAs by APH(2″)-Ia was monitored using the absorbance of NADH at 340 nM (ε = 6220 $M^{-1}cm^{-1}$) by the enzyme-coupled response to the production of GDP. Reactions (200 μL) contained PA (100 μM), Tris-HCl (50 mM, pH 8.0), $MgCl_2$ (10 mM), KCl (40 mM), NADH (0.5 mg mL^{-1}), PEP (2.5 mM), GTP (2 mM), PK/LDH (4 μL), and reactions were initiated by the addition of APH(2″) (1 μM). Reactions were monitored every 30 s for 30 min, and initial rates were determined using the first 2–5 min of reaction time.

Supplementary Material

Refer to Web version on PubMed Central for supplementary material.

Acknowledgments

This research was supported by National Institute of Health grants (1R41GM100607, 2R42GM100607) to D. P. Arya and (1R01AI090048) to S. Garneau-Tsodikova, and support from NASA astrobiology institute NNA09DA78A to A. K. Oyelere. We thank T. McNealy (Clemson University; Clemson, South Carolina) for the *S. aureus* (ATCC 25923) and *S. pyogenes* (ATCC 12384) strains.

References

1. Houghton JL, Green KD, Chen W, Garneau-Tsodikova S. The Future of Aminoglycosides: the End or Renaissance? ChemBioChem. 2010; 11:880–902. [PubMed: 20397253]
2. Yang L, Ye X. Development of aminoglycoside antibiotics effective against resistant bacterial strains. Curr Top Med Chem. 2010; 10:1898–1826. [PubMed: 20615188]
3. Moazed D, Noller HF. Interaction of antibiotics with functional sites in 16S ribosomal RNA. Nature. 1987; 327:389–394. [PubMed: 2953976]
4. Purohit P, Stern S. Interactions of a small RNA with antibiotic and RNA ligands of the 30S subunit. Nature. 1994; 370:659–662. [PubMed: 8065453]
5. Fourmy D, Recht MI, Blanchard SC, Puglisi JD. Structure of the A site of *Escherichia coli* 16S ribosomal RNA complexed with an aminoglycoside antibiotic. Science. 1996; 274:1367–1371. [PubMed: 8910275]
6. Tor Y. The ribosomal A-site as an inspiration for the design of RNA binders. Biochimie. 2006; 88:1045–1051. [PubMed: 16581175]
7. Chambers HF, DeLeo FR. Waves of resistance: *Staphylococcus aureus* in the antibiotic era. Nat Rev Microbiol. 2009; 7:629–641. [PubMed: 19680247]
8. Bera S, Zhanel GG, Schweizer F. Evaluation of amphiphilic aminoglycoside-peptide triazole conjugates as antibacterial agents. Bioorg Med Chem Lett. 2010; 20:3031–3035. [PubMed: 20413307]
9. Bera S, Zhanel GG, Schweizer F. Antibacterial activities of aminoglycoside antibiotic-derived cationic amphiphiles: Polyol-modified neomycin B-, kanamycin A-, amikacin-, and neamine-based amphiphiles with potent broad spectrum antibacterial activity. J Med Chem. 2010; 53:3626–3631. [PubMed: 20373816]
10. Findlay B, Zhanel GG, Schweizer F. Neomycin-phenolic conjugates: polycationic amphiphiles with broad-spectrum antibacterial activity, low hemolytic activity and weak serum protein binding. Bioorg Med Chem Lett. 2012; 22:1499–1503. [PubMed: 22285320]
11. Zhang J, Chiang FI, Wu L, Czyryca PG, Li D, Chang CT. Surprising Alteration of Antibacterial Activity of 5″-Modified Neomycin against Resistant Bacteria. J Med Chem. 2008; 51:7563–7573. [PubMed: 19012394]
12. Fridman M, Belakhov V, Yaron S, Baasov T. A new class of branched aminoglycosides: pseudo-pentasaccharide derivatives of neomycin B. Org Lett. 2003; 5:3575–3578. [PubMed: 14507176]
13. Hainrichson M, Pokrovskaya V, Shallom-Shezifi D, Fridman M, Belakhov V, Shachar D, Yaron S, Baasov T. Branched aminoglycosides: biochemical studies and antibacterial activity of neomycin B derivatives. Biorg Med Chem. 2005; 13:5797–5807.
14. Sitaram N, Nagaraj R. Interaction of antimicrobial peptides with biological and model membranes: structural and charge requirements for activity. Biochim Biophys Acta. 1999; 1462:29–54. [PubMed: 10590301]
15. Dathe M, Wieprecht T. Structural features of helical antimicrobial peptides: their potential to modulate activity on model membranes and biological cells. Biochim Biophys Acta. 1999; 1462:71–87. [PubMed: 10590303]
16. Hancock REW, Rozek A. Role of membranes in the activities of antimicrobial cationic peptides. FEMS Microbiol Lett. 2002; 206:143–149. [PubMed: 11814654]
17. Fosso MY, Li Y, Garneau-Tsodikova S. New trends in aminoglycosides use. MedChemComm. 2014; 5:1075–1091. [PubMed: 25071928]
18. Kumar S, Spano MN, Arya DP. Shape readout of AT rich DNA by carbohydrates. Biopolymers. 2013; 101:720–732. [PubMed: 24281844]

19. Hamilton PL, Arya DP. Natural product DNA major groove binders. Nat Prod Rep. 2012; 29:134–143. [PubMed: 22183179]
20. Xi H, Davis E, Ranjan N, Xue L, Hyde-Volpe D, Arya DP. Thermodynamics of nucleic Acid "shape readout" by an aminosugar. Biochemistry. 2011; 50:9088–9113. [PubMed: 21863895]
21. Willis B, Arya DP. An expanding view of aminoglycoside-nucleic acid recognition. Adv Carbohydr Chem Biochem. 2006; 60:251–302. [PubMed: 16750445]
22. Bera S, Zhanel GG, Schweizer F. Design, synthesis, and antibacterial activities of neomycin-lipid conjugates: polycationic lipids with potent Gram-positive activity. J Med Chem. 2008; 51:6160–6164. [PubMed: 18778047]
23. Bera S, Zhanel GG, Schweizer F. Antibacterial activity of guanidinylated neomycin B- and kanamycin A-derived amphiphilic lipid conjugates. J Antimicrob Chemother. 2010; 65:1224–1227. [PubMed: 20332193]
24. Bera S, Zhanel GG, Schweizer F. Synthesis and antibacterial activity of amphiphilic lysine-ligated neomycin B conjugates. Carbohydr Res. 2011; 346:560–568. [PubMed: 21353205]
25. Kumar S, Arya DP. Recognition of HIV TAR RNA by triazole linked neomycin dimers. Bioorg Med Chem Lett. 2011; 21:4788–4792. [PubMed: 21757341]
26. Xue L, Ranjan N, Arya DP. Synthesis and spectroscopic studies of the (neomycin)-perylene conjugate binding to human telomeric DNA. Biochemistry. 2011; 50:2838–2849. [PubMed: 21329360]
27. Willis B, Arya DP. Triple recognition of B-DNA by a neomycin-Hoechst 33258-pyrene conjugate. Biochemistry. 2010; 49:452–469. [PubMed: 20000367]
28. Xue L, Xi H, Kumar S, Gray D, Davis E, Hamilton P, Skriba M, Arya DP. Probing the recognition surface of a DNA triplex: binding studies with intercalator-neomycin conjugates. Biochemistry. 2010; 49:5540–5552. [PubMed: 20499878]
29. Shaw NN, Xi H, Arya DP. Molecular recognition of a DNA:RNA hybrid: sub-nanomolar binding by a neomycin-methidium conjugate. Bioorg Med Chem Lett. 2008; 18:4142–4145. [PubMed: 18573660]
30. Willis B, Arya DP. Recognition of B-DNA by neomycin-Hoechst 33258 conjugates. Biochemistry. 2006; 45:10217–10232. [PubMed: 16922497]
31. Charles I, Arya DP. Synthesis of neomycin-DNA/peptide nucleic acid conjugates. J Carbohydr Chem. 2005; 24:145–160.
32. Arya DP, Coffee RL Jr, Xue L. From triplex to B-form duplex stabilization: reversal of target selectivity by aminoglycoside dimers. Bioorg Med Chem Lett. 2004; 14:4643–4646. [PubMed: 15324880]
33. Arya DP, Willis B. Reaching into the major groove of B-DNA: synthesis and nucleic acid binding of a neomycin-hoechst 33258 conjugate. J Am Chem Soc. 2003; 125:12398–12399. [PubMed: 14531669]
34. Arya DP, Xue L, Tennant P. Combining the best in triplex recognition: synthesis and nucleic acid binding of a BQQ-neomycin conjugate. J Am Chem Soc. 2003; 125:8070–8071. [PubMed: 12837054]
35. Coin I, Beyermann M, Bienert M. Solid-phase peptide synthesis: from standard procedures to the synthesis of difficult sequences. Nat Protoc. 2007; 2:3247–3256. [PubMed: 18079725]
36. Michael K, Wang H, Tor Y. Enhanced RNA binding of dimerized aminoglycosides. Biorg Med Chem. 1999; 7:1361–1371.
37. Boer J, Blount KF, Luedtke NW, Elson-Schwab L, Tor Y. RNA-selective modification by a platinum(II) complex conjugated to amino- and guanidinoglycosides. Angew Chem, Int Ed. 2005; 44:927–932.
38. Quader S, Boyd SE, Jenkins ID, Houston TA. Multi-site modification of neomycin B: combined mitsunobu and click chemistry approach. J Org Chem. 2007; 72:1962–1979. [PubMed: 17298096]
39. Kumar S, Kellish P, Robinson WE, Wang D, Appella DH, Arya DP. Click dimers to target HIV TAR RNA conformation. Biochemistry. 2012; 51:2331–2347. [PubMed: 22339203]
40. Watkins D, Norris FA, Kumar S, Arya DP. A fluorescence-based screen for ribosome binding antibiotics. Anal Biochem. 2013; 434:300–307. [PubMed: 23262284]

41. Zhao F, Zhao Q, Blount K, Han Q, Tor Y, Hermann T. Molecular recognition of RNA by neomycin and a restricted neomycin derivative. Angew Chem, Int Ed. 2005; 44:5329–5334.
42. Ryu D, Rando R. Aminoglycoside binding to human and bacterial A-site rRNA decoding region constructs. Bioorg Med Chem. 2001; 9:2601–2608. [PubMed: 11557348]
43. De La Fuente R, Sonawane ND, Arumainayagam D, Verkman AS. Small molecules with antimicrobial activity against E. coli and P. aeruginosa identified by high-throughput screening. Br J Pharmacol. 2006; 149:551–559. [PubMed: 16981005]
44. King A, Watkins D, Kumar S, Ranjan N, Gong C, Whitlock J, Arya DP. Characterization of ribosomal binding and antibacterial activities using two orthogonal high-throughput screens. Antimicrob Agents Chemother. 2013; 57:4717–4726. [PubMed: 23856777]
45. Shaul P, Green KD, Rutenberg R, Kramer M, Berkov-Zrihen Y, Breiner-Goldstein E, Garneau-Tsodikova S, Fridman M. Assessment of 6′- and 6‴-N-acylation of aminoglycosides as a strategy to overcome bacterial resistance. Org Biomol Chem. 2011; 9:4057–4063. [PubMed: 21365081]
46. Sucheck SJ, Wong AL, Koeller KM, Boehr DD, Draker K, Sears P, Wright GD, Wong C. Design of Bifunctional Antibiotics that Target Bacterial rRNA and Inhibit Resistance-Causing Enzymes. J Am Chem Soc. 2000; 122:5230–5231.
47. Chen W, Biswas T, Porter VR, Tsodikov OV, Garneau-Tsodikova S. Unusual regioversatility of acetyltransferase Eis, a cause of drug resistance in XDR-TB. Proc Natl Acad Sci U S A, Early Ed. 2011; 1–5:5.
48. Green KD, Chen W, Houghton JL, Fridman M, Garneau-Tsodikova S. Exploring the substrate promiscuity of drug-modifying enzymes for the chemoenzymatic generation of N-acylated aminoglycosides. ChemBioChem. 2010; 11:119–126. [PubMed: 19899089]
49. Green KD, Chen W, Garneau-Tsodikova S. Effects of altering aminoglycoside structures on bacterial resistance enzyme activities. Antimicrob Agents Chemother. 2011; 55:3207–3213. [PubMed: 21537023]
50. Daigle DM, Hughes DW, Wright GD. Prodigious substrate specificity of AAC(6′)-APH(2″), an aminoglycoside antibiotic resistance determinant in enterococci and staphylococci. Chem Biol. 1999; 6:99–110. [PubMed: 10021417]
51. Ogle JM, Brodersen DE, Clemons WM Jr, Tarry MJ, Carter AP, Ramakrishnan V. Recognition of cognate transfer RNA by the 30s ribosomal subunit. Science. 2001; 292:897–902. [PubMed: 11340196]
52. Lynch SR, Puglisi JD. Structural Origins of Aminoglycoside Specificity for Prokaryotic Ribosomes. J Mol Biol. 2001; 306:1037–1058. [PubMed: 11237617]
53. Barbieri CM, Kaul M, Bozza-Hingos M, Zhao F, Tor Y, Hermann T, Pilch DS. Defining the molecular forces that determine the impact of neomycin on bacterial protein synthesis: importance of the 2′-amino functionality. Antimicrob Agents Chemother. 2007; 51:1760–1769. [PubMed: 17353247]
54. Barbieri CM, Kaul M, Pilch DS. Use of 2-aminopurine as a fluorescent tool for characterizing antibiotic recognition of the bacterial rRNA A-site. Tetrahedron. 2007; 63:3567–6574. [PubMed: 18431442]
55. Cudic M, Lockatell CV, Johnson DE, L O Jr. In vitro and in vivo activity of an antibacterial peptide analog against uropathogens. Peptides. 2003; 24:807–820. [PubMed: 12948832]
56. Trott O, Olson AJ. AutoDock Vina: Improving the Speed and Accuracy of Docking with a New Scoring Function, Efficient Optimization, and Multithreading. J Comput Chem. 2010; 31:455–461. [PubMed: 19499576]
57. Sanner MF. Python: a programming language for software integration and development. J Mol Graphics & Modelling. 1999; 17:57–61.
58. Brunger A, Adams P, Clore G, DeLano W, Gros P, Grosse-Kunstleve R, Jiang J, Kuszewski J, Nilges M, Pannu N, Read R, Rice L, Simonson T, Warren G. Crystallography & NMR system: A new software suite for macromolecular structure determination. Acta Crystallogr, Sect D: Biol Crystallogr. 1998; 54:905–921. [PubMed: 9757107]
59. Pratt SD, David CA, Black-Schaefer C, Dandliker PJ, Xuei X, Warrior U, Burns DJ, Zhong P, Cao Z, Saiki AY, Lerner CG, Chovan LE, Soni NB, Nilius AM, Wagenaar FL, Merta PJ, Traphagen LM, Beutel BA. A strategy for discovery of novel broad-spectrum antibacterials using a

highthroughput *Streptococcus pneumoniae* transcription/translation screen. J Biomol Screen. 2004; 9:3–11. [PubMed: 15006143]

60. Thorne CA, Lafleur B, Lewis M, Hanson AJ, Jernigan KK, Weaver DC, Huppert KA, Chen TW, Wichaidit C, Cselenyi CS, Tahinci E, Meyers KC, Waskow E, Orton D, Salic A, Lee LA, Robbins DJ, Huppert SS, Lee E. A biochemical screen for identification of small-molecule regulators of the Wnt pathway using Xenopus egg extracts. J Biomol Scr. 2011; 16:995–1006.

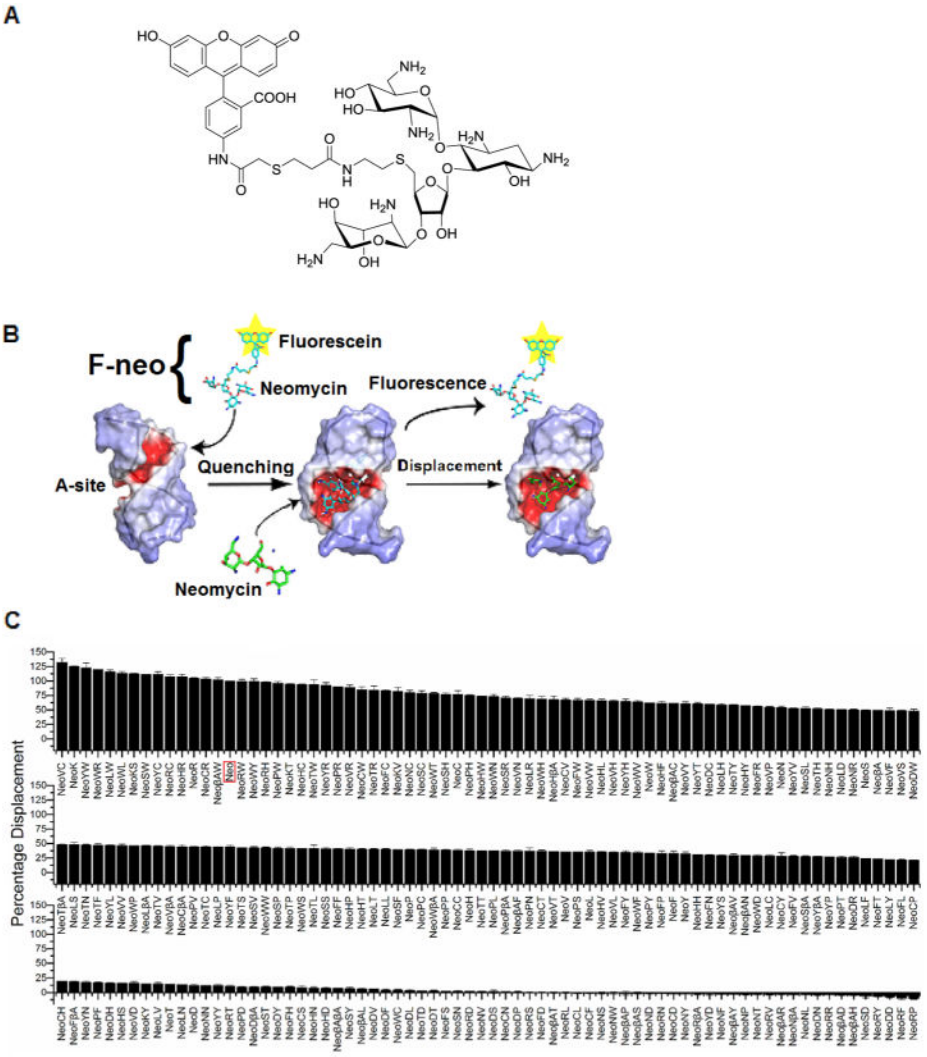

Figure 1.

(A) Structure of F-neo reporter molecule. (B) Schematic of the displacement assay of F-neo (cyan) by a competing ligand (neomycin; green) from the model ribosomal A-site (red and blue). The yellow star indicates fluorescence. (C) Ribosomal RNA A-site binding screening results of 215 neomycin-amino acid conjugates. The percentage displacement of neomycin was determined as described in eq 1. Neomycin (Neo) is shown in a red box and was set to 100%. The bindings of all other compounds are relative to the binding of neomycin. Each experiment was performed in duplicate, and standard deviation in the measurement is shown as error bars for each compound. The assay was performed with each compound at a 0.3 μM concentration to 0.1 μM F-neo:A-site complex using 100 reads per well at an excitation/emission of 485/535 nm. All experiments were performed in duplicate in 10 mM MOPSO (pH 7.0), 50 mM NaCl, and 0.4 mM EDTA.

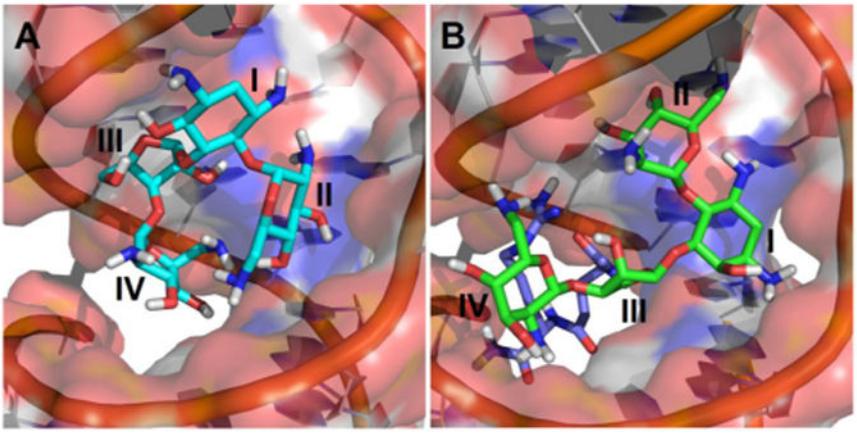

Figure 2.

Docking of neomycin and NeoR (DPA1102) onto the *E. coli* ribosomal A-site. Neomycin (A: cyan sticks) and NeoR (B: green and blue sticks) were docked onto a model of the ribosomal A-site (partially transparent surface overlaid onto a cartoon representation) using Autodock Vina. Similar to the crystal structure, ring II of neomycin in panel A is below ring I and closer to the unstacked adenines. The neomycin moiety (green sticks) in panel B has ring II below ring I and closer to the unstacked adenines. The amino acid side chain (blue sticks) is between the floor of the groove and rings III and IV. The *E. coli* ribosomal A-site was modeled from the crystal structure of neomycin in complex with the A-site (PDB ID: 2A04).[41]

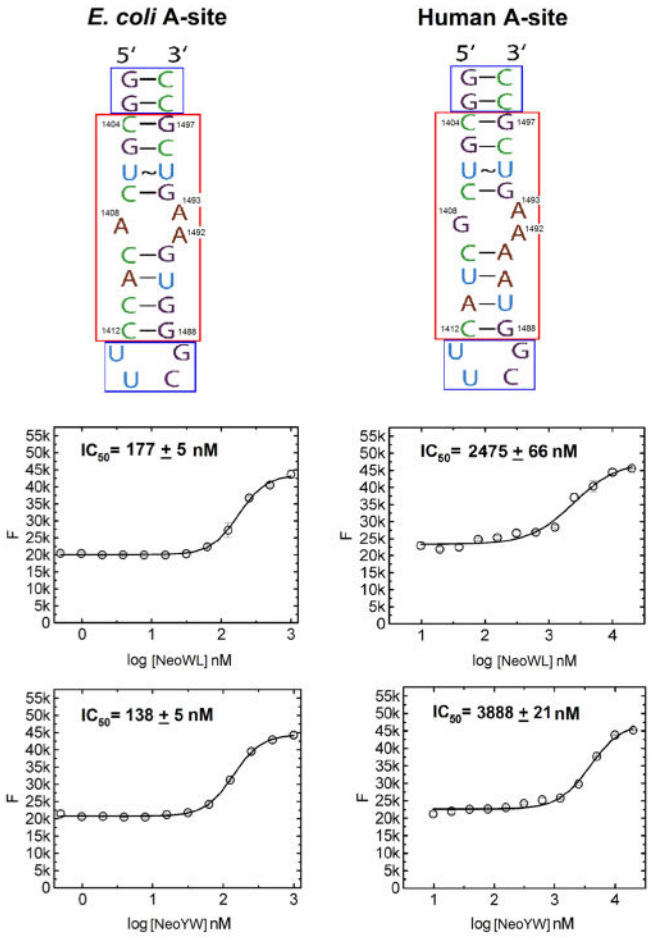

Figure 3.

PA compounds that discriminate between the *E. coli* and human model A-site. The secondary structure of the model A-site used in the development of the high throughput screen is shown at the top. The red box indicates the residues that are present in the *E. coli* or human rRNA and are numbered according to the *E. coli* ribosome. Compounds DPA1199 (NeoWL) and compound DPA1308 (NeoYW) bind to the *E. coli* A-site (left) 14–28 times stronger than to human A-site (right).

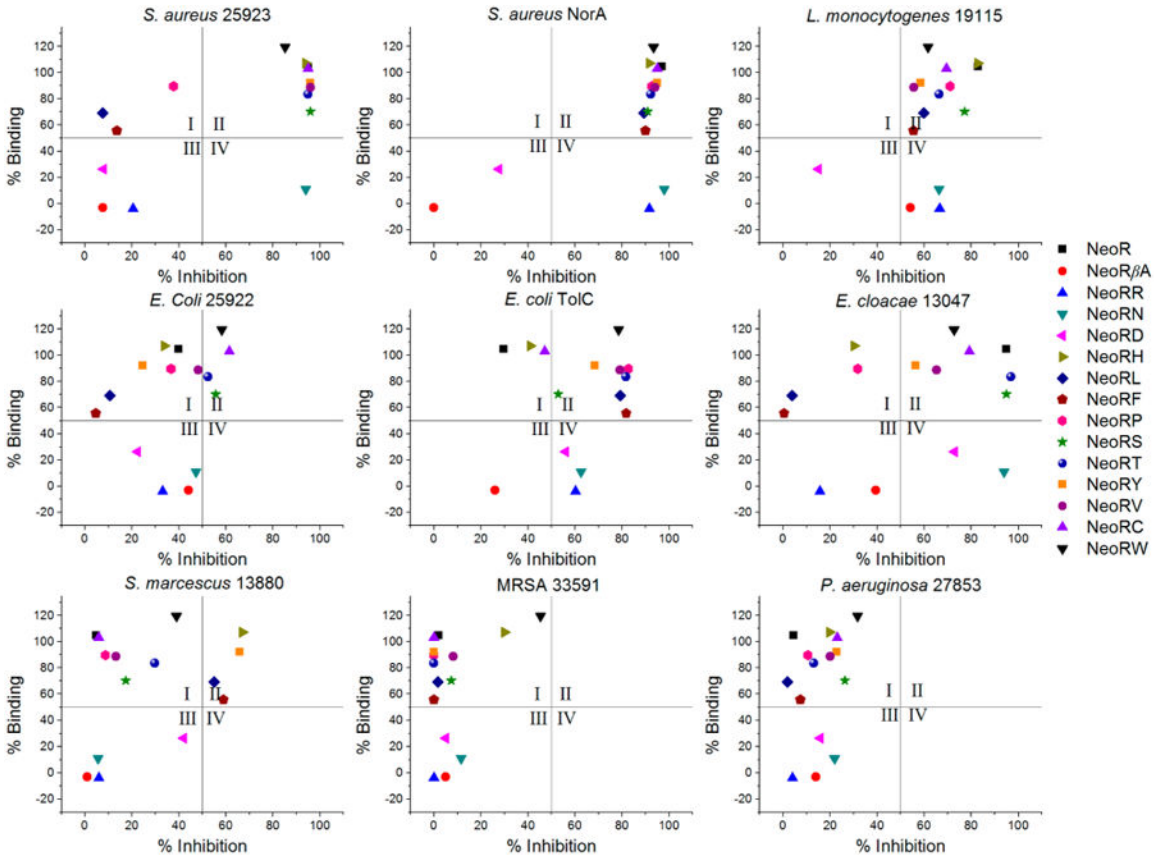

Figure 4.
RB-BIP of neomycin amino acid compounds with arginine on conjugate position 1.

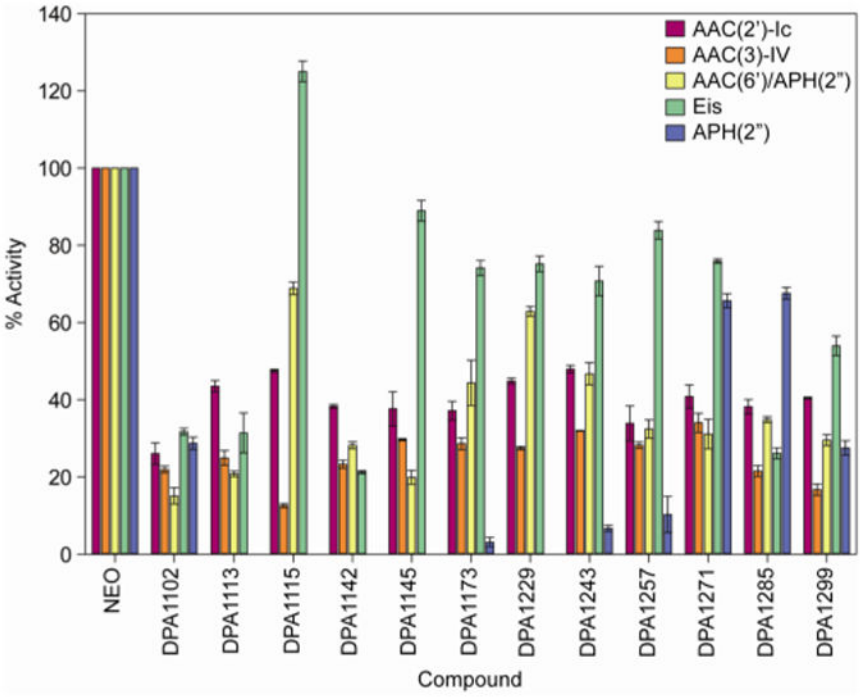

Figure 5.
PA conjugates tested against a variety of aminoglycoside-modifying enzymes.

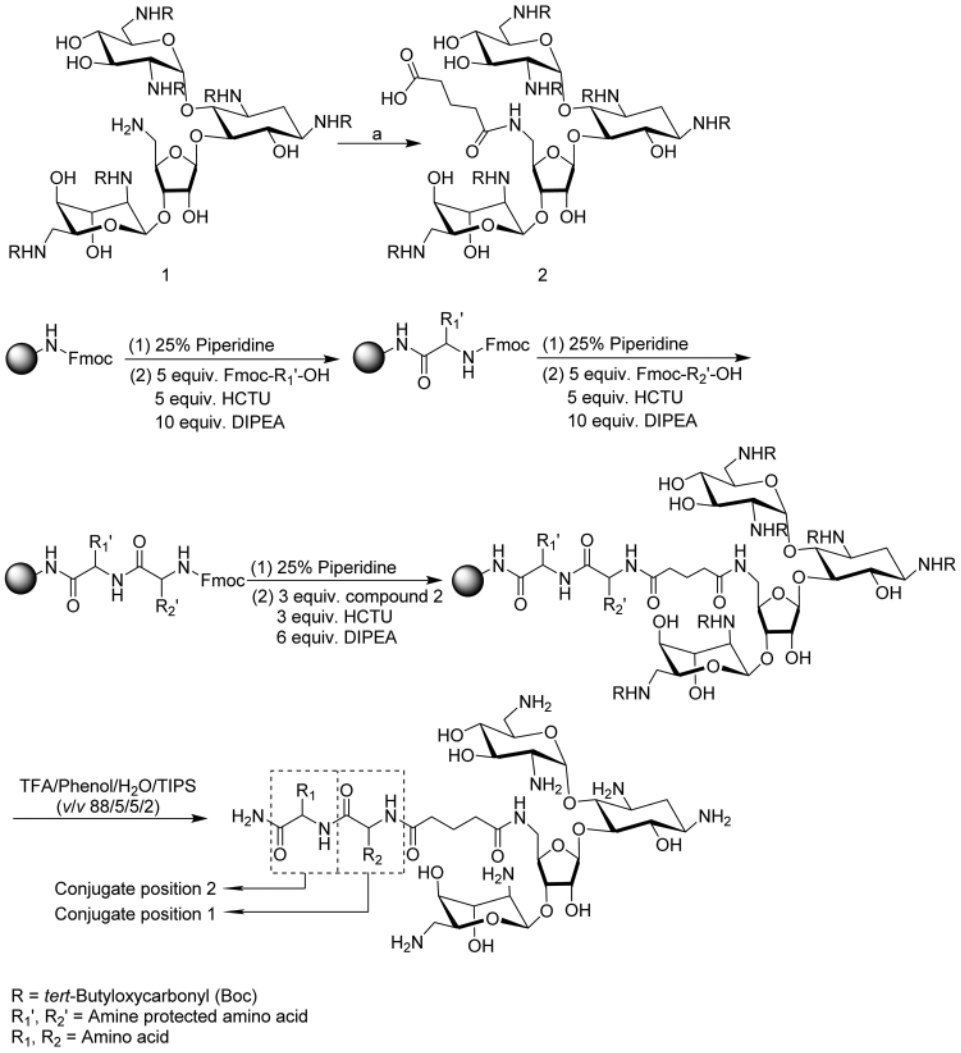

Scheme 1. Synthesis of Neomycin-Amino-Acid Conjugates[a]

[a]Reagents and conditions: (a) glutaric anhydride, Et_3N, DMF, r.t., 95%.

Table 1

A-site Binding Analysis[a]

Position 2		Position 1														
		Positive		Polar					Negative	Aromati			Non-Polar			
		R	K	H	N	C	S	T	D	W	Y	F	βA	V	L	P
	N/A	105	125	39	54	76	52	15	14	62	33	33	51	36	35	40
Positive	R	0	-	97	0	107	1	12	2	99	0	0	0	0	0	0
Polar	H	107	-	33	8	94	17	41	7	74	57	61	67	35	65	41
	N	11	-	53	13	80	0	0	0	0	0	0	0	2	0	0
	C	103	-	21	1	39	9	37	0	85	29	0	46	67	0	22
	S	70	112	77	2	78	41	9	0	111	7	40	28	44	36	42
	T	84	94	53	48	45	44	38	3	93	58	48	49	47	41	42
Negative	D	26	-	17	0	59	2	3	0	49	9	6	9	6	4	1
Aromatic	W	120	-	68	73	4	42	78	29	44	99	35	39	63	113	47
	Y	92	16	64	19	111	31	60	0	122	12	44	28	54	48	27
	F	56	-	9	32	83	2	26	0	67	35	41	21	28	23	34
Non-Polar	βA	0	-	0	29	61	0	0	0	102	0	37	7	30	6	0
	V	89	81	65	70	132	50	37	16	66	61	50	46	48	35	45
	L	69	-	58	14	29	49	41	0	116	24	26	47	16	40	44
	P	90	-	75	37	40	36	27	12	96	34	19	37	46	38	39
Color coding [*] =			+2	+1	0	-1	-2	Zwitter								

[a]The compounds were analyzed based on the charge on individual amino acids.

The numbers are the percentage displacement of F-neo from an A-site/F-neo complex by peptidic neomycin as shown in Figure 1C for each DPA numbered compound as a function of each amino acid(s) conjugated. The third row gives the one-letter code of the amino acid on the conjugate position 1 (firstly conjugated to neomycin). The second column gives the one-letter code of the amino acid on conjugate position 2 (secondly conjugated to neomycin). Results are color coded as total charges of the amino acids on peptidic neomycin.

[*]Total charges of the amino acids on peptidic neomycin under physiological pH. Zwitter indicates that the peptidic neomycin contains an amino acid with a positively charged side chain and an amino acid with a negatively charged side chain.

ACS Chem Biol. Author manuscript; available in PMC 2016 May 15.

Table 2

Favored Amino Acids from Antibacterial Screening at 5 μM

	Screened Target	Compounds σ averaged over all variations at position 2 with constant amino acids at position 1														
		NeoRX	**NeoKX**	**NeoHX**	**NeoNX**	**NeoPX**	**NeoYX**	**NeoSX**	**NeoWX**	**NeoTX**	**NeoβAX**	**NeoCX**	**NeoFX**	**NeoLX**	**NeoVX**	**NeoDX**
Gram-positive	*S. aureus* ATCC 25923	2.26	0.09	-0.21	-0.07	-0.40	-0.10	-0.17	-0.11	-0.14	-0.23	0.68	-0.31	-0.26	-0.41	-0.56
	S. aureus NorA	2.28	1.12	0.12	-0.30	-0.47	-0.39	-0.11	0.26	-0.30	-0.26	0.69	-0.50	-0.47	-0.41	-0.53
	MRSA ATCC 33591	0.02	-0.20	0.24	-0.16	-0.29	-0.08	0.12	1.02	0.14	0.19	0.12	-0.47	-0.29	-0.24	-0.26
	L. monocytogenes ATCC 19115	1.98	1.32	0.30	-0.10	-0.43	-0.36	0.06	-0.29	-0.12	-0.15	0.82	-0.49	-0.50	-0.50	-0.65
Gram-Negative	*E.coli* ATCC 25922	2.02	2.13	-0.29	-0.23	-0.37	-0.07	0.00	0.03	0.00	-0.34	-0.05	-0.35	-0.19	-0.35	-0.53
	E. coli TolC	0.74	0.82	0.18	-0.17	-0.46	0.22	0.18	0.96	-0.12	-0.34	0.12	-0.20	-0.14	-0.19	-1.05
	E. cloacae ATCC 13047	2.54	0.98	-0.02	-0.35	-0.33	-0.14	0.02	-0.21	-0.27	-0.29	0.08	-0.35	-0.36	-0.28	-0.36
	S. marcescens ATCC 13880	2.08	-0.38	-0.34	-0.13	-0.41	-0.04	-0.29	0.41	-0.09	-0.39	0.28	-0.20	-0.18	-0.25	-0.33
	P. aeruginosa ATCC 27853	0.01	0.09	-0.47	-0.08	-0.49	-0.06	-0.44	0.91	0.09	-0.50	1.04	-0.14	0.33	-0.01	-0.22
	Screened Target	Compounds σ averaged over all variations at position 1 with constant amino acids at position 2														
		NeoXR	NeoXK	NeoXH	NeoXN	NeoXP	NeoXY	NeoXS	NeoXW	NeoXT	NeoXβA	NeoXC	NeoXF	NeoXL	NeoXV	NeoXD
Gram-positive	*S. aureus* ATCC 25923	-0.02	-	0.00	0.02	0.13	0.16	0.40	-0.05	0.09	-0.50	0.01	0.05	-0.26	0.29	-0.46
	S. aureus NorA	0.81	-	-0.14	0.00	-0.20	0.12	0.07	-0.02	-0.38	-0.22	-0.08	-0.10	-0.22	-0.07	-0.27
	MRS A ATCC 33591	-0.25	-	-0.09	-0.01	-0.13	-0.14	-0.01	1.09	0.36	-0.23	-0.32	-0.15	-0.17	0.28	0.24
	L. monocytogenes ATCC 19115	0.81	-	0.89	-0.29	-0.26	-0.40	0.46	-0.45	0.02	-0.40	0.01	-0.45	-0.20	-0.27	-0.63
Gram-negative	*E coli* ATCC 25922	0.45	-	-0.10	-0.01	-0.09	-0.16	0.32	0.21	0.05	-0.07	-0.30	-0.49	-0.70	-0.09	-0.23
	E. coli TolC	-0.27	-	-0.24	-0.23	0.40	0.22	0.49	0.74	-0.78	-0.61	-0.39	0.77	0.26	0.24	-0.57
	E. cloacae ATCC 13047	0.10	-	-0.17	0.06	-0.34	-0.01	0.04	0.04	-0.07	-0.11	0.07	-0.26	-0.36	-0.13	-0.06
	S. marcescens ATCC 13880	-0.29	-	0.34	-0.20	0.01	0.26	-0.14	0.86	0.06	-0.42	-0.21	0.43	0.16	-0.11	0.01
	P. aeruginosa ATCC 27853	-0.54	-	-0.53	-0.37	0.55	0.35	0.72	1.14	0.16	-0.87	0.43	-0.32	-0.57	0.35	0.00

	Screened Target	Compounds σ averaged over all variations at position 2 with constant amino acids at position 1													
		NeoRX	**NeoKX**	**NeoHX**	**NeoNX**	**NeoPX**	**NeoYX**	**NeoSX**	**NeoWX**	**NeoTX**	**NeoβAX**	**NeoCX**	**NeoFX**	**NeoLX**	**NeoVX**	**NeoDX**
Color coding* =		σ ≥ 1			1 > σ ≥ 0.5			-0.5 ≥ σ > -1			σ ≤ -1					

*The average inhibition and standard deviation from the mean (σ) was taken for all compounds in the library. The σ for the inhibition was determined for each compound. The average σ for all compounds with the indicated amino acid at postion 1 (2) was determined for all compound variations (X) at position 2 (1).

Table 3

Minimal Inhibitory Concentration (MIC) in μM

		bacterial strains (μM)									
name	**DPA no.**	**A**	**B**	**C**	**D**	**E**	**F**	**G**	**H**	**I**	**J**
Neo		0.625	>320	>80	10	2.5	2.5	160	2.5	>320	80
NeoR	1102	1.25	>160	>80	10	5	20	80	1.25	>160	80
NeoC	1113	5	>160	>80	40	20	80	>160	5	>160	>80
NeoK	1115	5	>160	>80	40	20	80	>160	5	>160	>80
NeoCR	1142	10	>160	>80	40	80	>80	>160	5	>160	>80
NeoRN	1145	5	>160	>80	20	5	20	>160	2.5	>160	>80
NeoRH	1173	5	>160	>80	20	20	40	>160	5	>160	>80
NeoRS	1229	1.25	>160	>80	20	5	20	80	2.5	>160	80
NeoRT	1243	5	>160	>80	40	5	20	>160	5	>160	>80
NeoRY	1257	5	>160	>80	20	10	20	>160	2.5	>160	>80
NeoRV	1271	5	>160	>80	20	20	20	160	5	>160	80
NeoRC	1285	5	>160	>80	20	20	40	160	5	>160	>80
NeoRW	1299	10	>160	>80	20	>80	>80	160	10	>160	80

A = *S. aureus* ATCC 25923, **B** = MRSA ATCC 33591, **C** = *P. aeruginosa* ATCC 27853, **D** = *E. coli* ATCC 25922, **E** = *E. cloacae* ATCC 13047, **F** = *S. marcescens* ATCC 13880, **G** = *S. pyogenes* ATCC 12384, **H** = *S. aureus* NorA, **I** = *E. coli* TolC, **J** = *L. monocytogenes* ATCC 19115.

ACS Chem Biol. Author manuscript; available in PMC 2016 May 15.

Table 4

IC_{50} of PA Compounds for Cell Free Luciferase Inhibition Assay

compound	Neo	NeoK	NeoR	NeoRH	NeoRC	NeoRS	NeoRT	NeoRV	NeoRW	NeoRY	NeoC	NeoCR
IC_{50} (nM)[a]	24	262	34	226	104	34	56	73	58	56	118	246

[a]IC_{50} is the concentration of compound that inhibits the translation of luciferase as determined by the luciferase assay as described in the Materials and Methods. Fits and errors of measurements can be found in the Table S13 of Supporting Information.